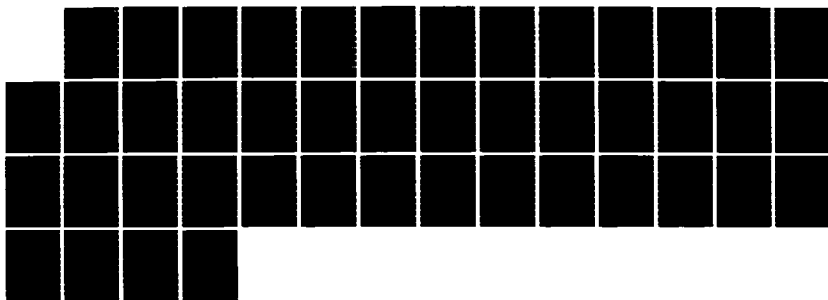


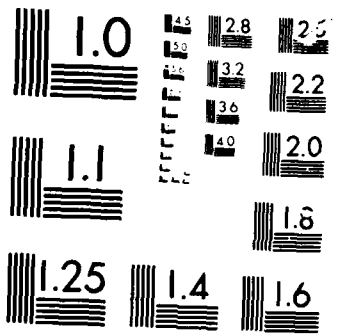
AD-A169 222 COCHLEAR MECHANICS: ANALYSIS OF THE TRANSIENT RESPONSE 1/1
(U) RENSSELAER POLYTECHNIC INST TROY NY DEPT OF
MATHEMATICAL SCIENCES M H HOLMES 01 MAR 86

UNCLASSIFIED RPI-MATH-154 ARO-28474.6-MA

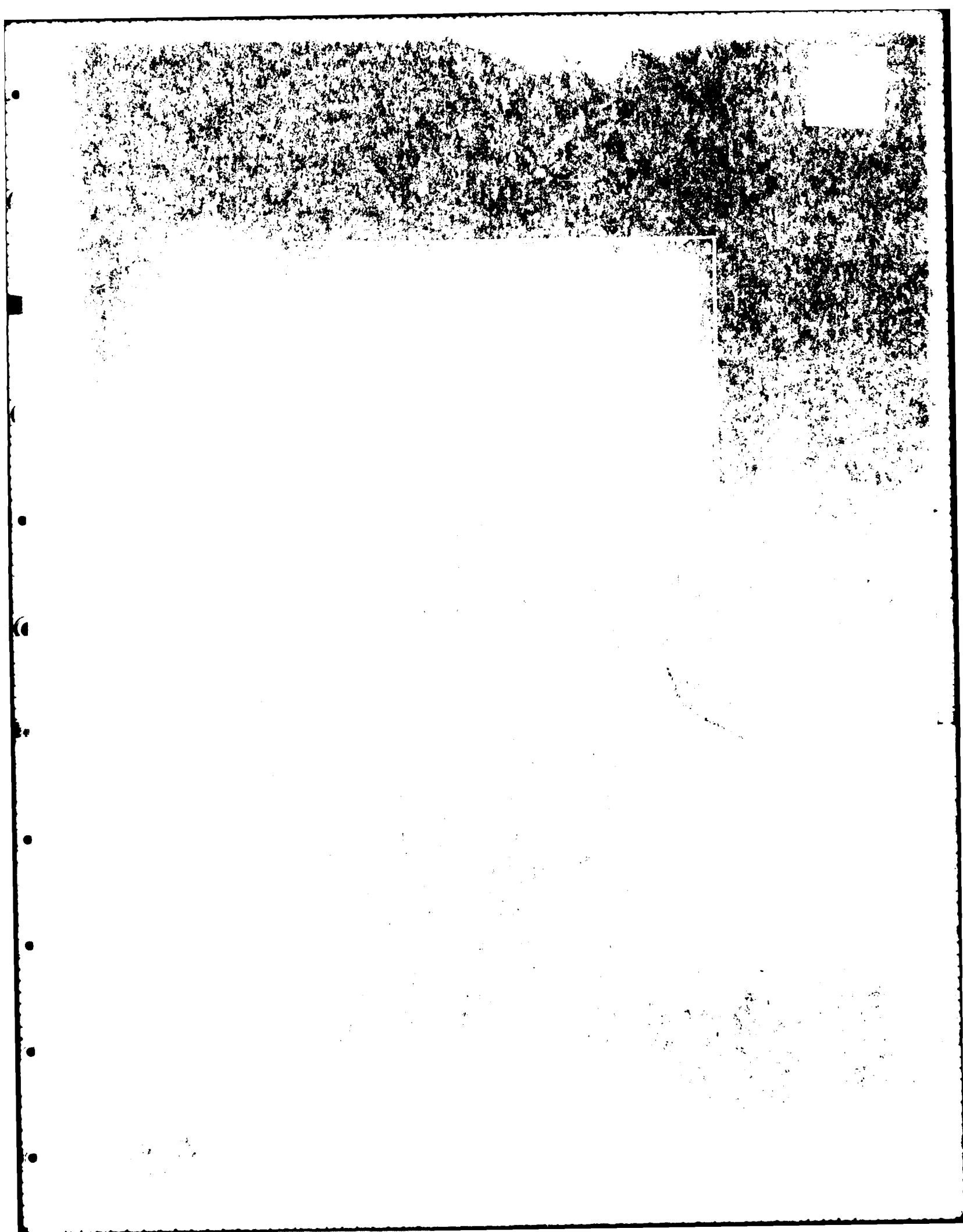
F/G 6/16

ML





MICROLINE



ARO 20474.6-MA

2

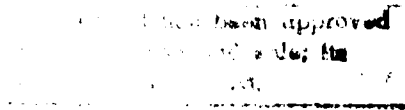
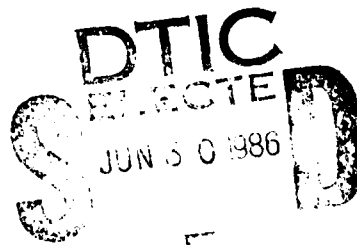
R.P.I. Math Report No. 154
March 1, 1986

COCHLEAR MECHANICS:
ANALYSIS OF THE TRANSIENT RESPONSE

by

Mark H. Holmes

Department of Mathematical Sciences
Rensselaer Polytechnic Institute
Troy, New York 12180-3590



This work was supported by the U.S. Army Research Office
contract number DAAG29-83-K-0092.

UNCLASSIFIED

SECURITY CLASSIFICATION OF THIS PAGE (When Data Entered)

REPORT DOCUMENTATION PAGE		READ INSTRUCTIONS BEFORE COMPLETING FORM
1. REPORT NUMBER ARO 20474.6-MA	2. GOVT ACCESSION NO. N/A	3. RECIPIENT'S CATALOG NUMBER N/A
4. TITLE (and Subtitle) Cochlear Mechanics: Analysis of the Transient Response		5. TYPE OF REPORT & PERIOD COVERED Technical Report
		6. PERFORMING ORG. REPORT NUMBER
7. AUTHOR(s) Mark H. Holmes		8. CONTRACT OR GRANT NUMBER(s) DAAG29-83-K-0092
9. PERFORMING ORGANIZATION NAME AND ADDRESS Rensselaer Polytechnic Institute Troy, NY 12180		10. PROGRAM ELEMENT, PROJECT, TASK AREA & WORK UNIT NUMBERS
11. CONTROLLING OFFICE NAME AND ADDRESS U. S. Army Research Office Post Office Box 12211 Research Triangle Park NC 27709		12. REPORT DATE March 1, 1986
14. MONITORING AGENCY NAME & ADDRESS (if different from Controlling Office)		13. NUMBER OF PAGES 40
		15. SECURITY CLASS. (of this report) Unclassified
		15a. DECLASSIFICATION/DOWNGRADING SCHEDULE
16. DISTRIBUTION STATEMENT (of this Report) Approved for public release; distribution unlimited.		
17. DISTRIBUTION STATEMENT (of the abstract entered in Block 20, if different from Report) NA		
18. SUPPLEMENTARY NOTES The view, opinions, and/or findings contained in this report are those of the author(s) and should not be construed as an official Department of the Army position, policy, or decision, unless so designated by other documentation.		
19. KEY WORDS (Continue on reverse side if necessary and identify by block number)		
20. ABSTRACT (Continue on reverse side if necessary and identify by block number) The hydroelastic model of the cochlea is used to analyze the transient response to a sound signal. Using the relatively high frequencies in the hearing range the equations are first reduced using viscous boundary layer theory. The reduced problem is solved by first applying the Fourier transform and then using the solution for a pure-tone signal. The response to a tone-pip is then studied and comparisons are made, when possible, with experiment. For example, the "ringing" observed in the displacement of the basilar membrane is seen in the model and the theory agrees reasonably well with the neural		

UNCLASSIFIED

SECURITY CLASSIFICATION OF THIS PAGE(When Data Entered)

20.

latency measurements.



UNCLASSIFIED

SECURITY CLASSIFICATION OF THIS PAGE(When Data Entered)

ABSTRACT

The hydroelastic model of the cochlea is used to analyze the transient response to a sound signal. Using the relatively high frequencies in the hearing range the equations are first reduced using viscous boundary layer theory. The reduced problem is solved by first applying the Fourier transform and then using the solution for a pure-tone signal. The response to a tone-pip is then studied and comparisons are made, when possible, with experiment. For example, the "ringing" observed in the displacement of the basilar membrane is seen in the model and the theory agrees reasonably well with the neural latency measurements.

TABLE OF CONTENTS

	<u>PAGE</u>
INTRODUCTION	1
EQUATIONS OF MOTION	4
BOUNDARY LAYER APPROXIMATION	10
SOLUTION OF REDUCED PROBLEM	15
SOLUTION OF TRANSIENT PROBLEM	18
APPLICATION TO THE HUMAN COCHLEA	20
DISCUSSION	29
REFERENCES	31
APPENDIX: EVALUATION OF THE KERNEL FUNCTION	33

INTRODUCTION

In the study of the transmission and resolution of the sound signal in the cochlea the behavior associated with the longtime response to a pure tone has received, by far, the most attention. This is understandable as the work on this aspect of the hearing process has been invaluable in the elucidation of the basic mechanisms underlying frequency discrimination. However, to be able to address questions connected with speech discrimination and noise induced hearing loss it is necessary to consider the transient behavior. Unfortunately, the effort that has been invested in this aspect of the hearing process has been limited. In terms of direct experimental observation of the transient response of the basilar membrane, Robles, et al (1976) is one of the only studies presently available. In fact, most of the experimental works on the transient problem give only indirect indications of the motion of the basilar membrane. This includes psychoacoustical tests, such as Stapells, et al (1982), and neural measurements, such as Anderson, et al (1970) and Pfeiffer and Kim (1972). The modeling efforts are also limited and the few that have appeared in the literature have concentrated almost exclusively on the low frequency response. In fact, there has never been a complete analysis of the fully three dimensional transient motion in the cochlea.

It is for these reasons that the objective of the present study is to develop a description of the transient behavior in the cochlea that covers the entire hearing range. The model that is used for the cochlea is the same as the one that has been used to

describe the response to a pure tone (Holmes and Cole, 1983, 1984; Holmes, 1986). The formulation of the model is relatively simple and it assumes the fluid filling the chambers is viscous and incompressible and the basilar membrane is modeled as a fibrous elastic plate. Except for the fluid's density and viscosity, and the transverse elastic modulus and mass density for the basilar membrane, all of the parameters in the model are geometric. The values for these four parameters are known from independent tests so the model of the mammalian cochlea used here is characterized entirely by the geometric structure of the ear. Because of this the model can be applied easily to a wide variety of mammalian cochlae (Holmes, 1986).

In the next section the equations governing the motion in the cochlea are presented and nondimensionalized. The reason for scaling the problem is to simplify the analysis used to solve it. This is done by first using viscous boundary layer theory to reduce the problem. Once this is done a slender body approximation, which is based on the long narrow geometry of the cochlea, is used to obtain the solution of the problem. This is the same procedure that was used to study the response to a pure tone although the details of the derivation are somewhat different due to the time dependence of the problem. In any case, once the solution is derived it is then a simple matter to analyze the response of the basilar membrane to various signals.

The reason that viscous boundary layer theory can be used is because of the relative thinness of the layer as compared to the cross-sectional dimension of the fluid chamber. This should not be

interpreted to mean that the fluid viscosity is unimportant. In the model considered here the fluid viscosity is the only dissipative mechanism, and with it the theory gives a very accurate description of the frequency map, the moderate intensity amplitude and phase tuning curves, and the static stiffness measurements (Holmes, 1986). This includes human as well as other mammals (e.g., the cat, guinea pig, and chinchilla). At the same time, with the exceptions noted earlier, the parameters that define the model are all geometric and, as shown in Holmes (1985), they are determined solely from the measured values for each of these animals. This raises the question as to the importance of other possible dissipation mechanisms, such as membrane damping. Whatever contribution they make it is in addition to fluid viscosity. However, one of the difficulties with attempting to account for other damping mechanisms is that there are no direct experimental measurements on which to base the modeling assumptions. For example, there has never been a study of mode separation and transient amplitude decay for the basilar membrane. This makes the modeling effort almost guesswork, although one way around this is to assume that the damping mechanism is similar to that found in other fibrous biological membranes, such as the tympanic membrane (Rabbitt and Holmes, 1985). Except for Allen (1980) this has never been done and the usual assumption is that the damping is simply a dashpot mechanism. Such an assumption is difficult to justify as it has little basis in the ultrastructure of the basilar membrane or the organ of Corti.

EQUATIONS OF MOTION

The assumptions on the geometrical and structural components of the cochlea are similar to those made in Holmes and Cole (1984). Consequently, the presentation to follow is relatively brief but a more complete discussion of the assumptions made here can be found in the earlier paper. The cochlea is taken to be a tapered tube containing two fluid filled chambers (Fig. 1). The partition separating these chambers consists of a rigid section (the bony shelf), a flexible portion (the basilar membrane) and an aperture at the apical end (the helicotrema). The cochlear wall is rigid except at the basal end where there are two openings (the oval and round windows) that are covered by membranes. The footplate of the stapes is attached to the cochlea at the oval window. The variation of the geometry is fairly arbitrary except that it is assumed that the partition and basal end are planar surfaces and the cochlear wall is symmetric through the partition.

The fluid filling the two chambers is similar in terms of its mechanical behavior to water at body temperature. Accordingly, it is assumed to be an incompressible Newtonian fluid, and so, the equations of motion are

$$\left[\partial_t^* - \nu \nabla^2 \right] \vec{v}^* = - \frac{1}{\rho} \nabla p^* , \quad (1a)$$

and

$$\nabla \cdot \vec{v}^* = 0 , \quad (1b)$$

where $\vec{v}^*(x^*, y^*, z^*, t^*)$ is the velocity, $p^*(x^*, y^*, z^*, t^*)$ is the pressure, ν is the kinematic viscosity and ρ is the mass density. The asterisk appearing in (1) is used to distinguish the variables from their nondimensional analogs introduced below.

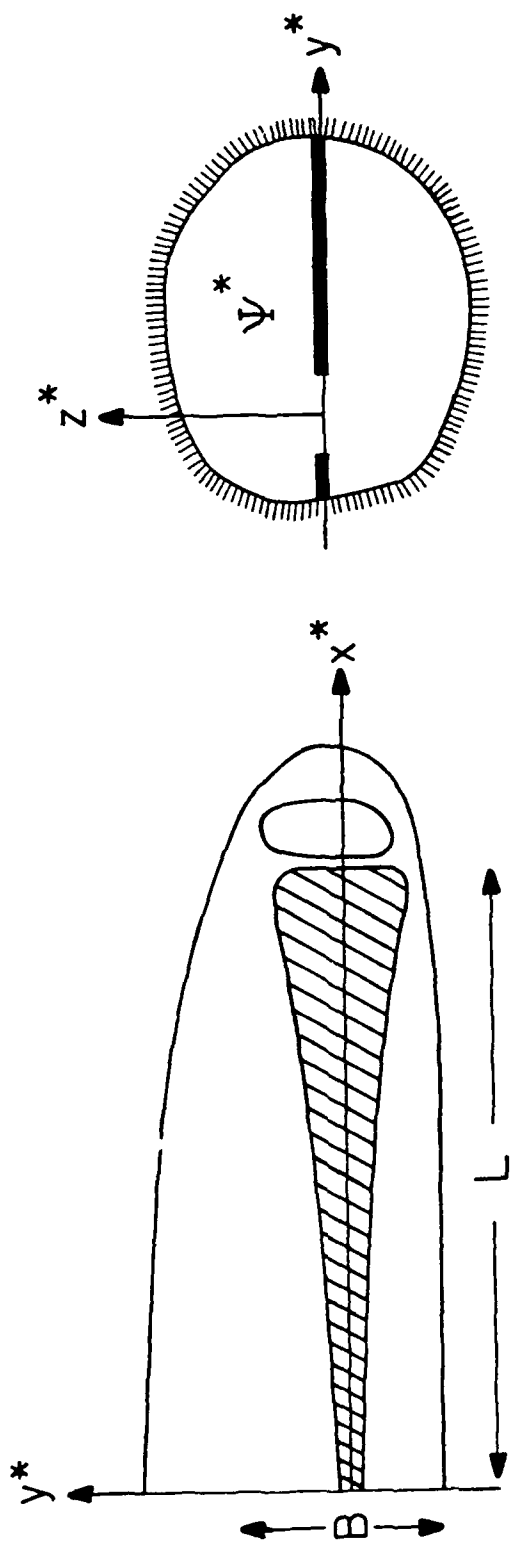
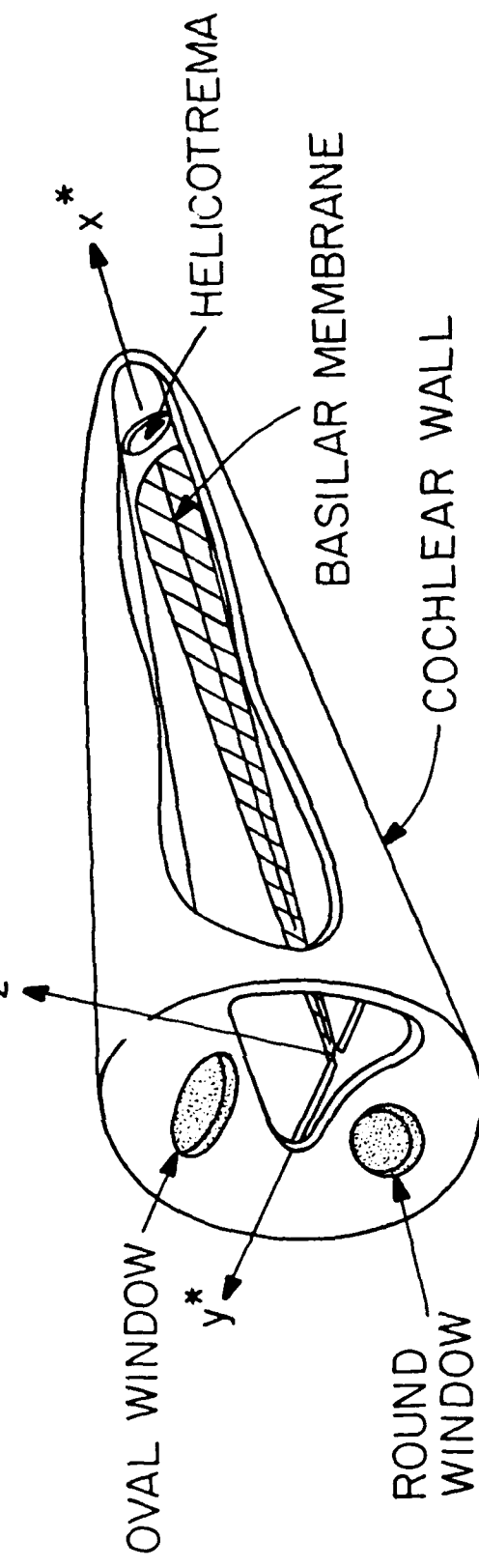


FIG. 1. The geometry and notation used for the hydroelastic model of the cochlea.

Also, the notation used here is the same as in Holmes and Cole (1984) except for the displacement of the stapes which is given in (4) below.

The basilar membrane (BM) is modeled as an inhomogeneous, strongly orthotropic, elastic plate. In this case the equation of motion is (Lekhnitskii, 1968)

$$D_2^* \partial_{y^*}^4 \eta^* + \mu^* \partial_{t^*}^2 \eta^* = - \left[p^*(x^*, y^*, 0, t^*) \right], \quad (1c)$$

where $\eta^*(x^*, y^*, t^*)$ is the displacement in the z^* -direction, D_2^* is the transverse bending rigidity, and μ^* is the mass per unit area of the basilar membrane. The longitudinal bending and twisting terms have not been included in (1c) as they have been found to be negligible in the basilar membrane (Voldrich, 1978; Holmes and Cole, 1984). The right-hand side of (1c) represents the fluid loading on the BM and is given as

$$\left[p^* \right] = p^*(x^*, y^*, 0^+, t^*) - p^*(x^*, y^*, 0^-, t^*). \quad (2)$$

By assuming the BM is inhomogeneous it is meant in (1c) that its material coefficients depend on the longitudinal variable x^* . Also note that the displacement of the basilar membrane is positive if it is in the positive z^* -direction.

To complete the description of the problem the boundary and initial conditions need to be specified. Because the fluid velocity must be continuous at the boundary we have that

$$\vec{v}^* = \begin{cases} \overset{\rightarrow}{0} & \text{on rigid wall} \\ (0, 0, \partial_{t^*} \eta^*) & \text{on BM} \end{cases}. \quad (3)$$

Similarly, at the oval and round windows

$$\vec{v}^* = (\partial_t \eta_s^*, 0, 0) , \quad (4)$$

where $\eta_s^*(t^*)$ represents the displacement of the stapes footplate. In (4), η_s^* is positive if it is in the positive x^* -direction. For the boundary conditions for the plate it is assumed that it is simply supported. It should be pointed out, however, that the methods used to solve the above problem do not depend on the particular boundary conditions for the basilar membrane and one could just as well assume it is clamped or clamped/simply supported (Holmes, 1986). As for initial conditions, it is assumed that the system starts from rest from its equilibrium position.

The transient problem for the cochlea is now complete and it involves solving the fluid equations (1a,b) coupled with the elastic boundary (1c). Given the three dimensional geometry and the relatively short waves that propagate along the basilar membrane even a numerical solution of this problem would be difficult as well as impractical at this time. However, the cochlea has a long slender geometry and the audible frequency range is relatively high. Both of these can be used to reduce the problem but to do so it is necessary to scale it. As in Holmes and Cole (1984) the spatial coordinates are nondimensionalized as follows

$$x^* = Lx, \quad y^* = By, \quad z^* = Bz,$$

where B, L are the width and length of the basilar membrane, respectively. Also, setting $t^* = t_C t$,

$$p^* = \left(\frac{\rho L \eta_{50}}{t_c^2} \right) p ,$$

$$\vec{v}^* = \frac{L \eta_{50}}{B t_c} \left(\frac{B}{L} v_1, v_2, v_3 \right) ,$$

and

$$\eta^* = \left(\frac{\rho L \eta_{50}}{u_c} \right) \eta , \quad (5)$$

where η_{50} is the amplitude of the stapes and u_c is a characteristic value for μ^* (e.g., it's value at $x=1/2$). The characteristic time scale t_c used here is

$$t_c^2 = \frac{B^* u_c}{D_{2c}} , \quad (6)$$

where D_{2c} is a characteristic value of D_2^* . Thus, t_c is a measure of the fundamental frequency of an elastic beam in a transverse cross-section of the basilar membrane. For example, for the human ear $t_c \sim 1.3$ msec. In Holmes and Cole (1984) the characteristic time scale was the driving frequency of the stapes. Although this differs from (6) the results of the analysis to follow actually contains this earlier work.

In dimensionless coordinates the problem describing the motion in the cochlea is:

i) fluid

$$(\partial_t - \delta^2 \nabla_\xi^2) \vec{v} = -\nabla p , \quad (7a)$$

$$\epsilon^2 \partial_x v_1 + \partial_y v_2 + \partial_z v_3 = 0 , \quad (7b)$$

ii) basilar membrane

$$D_2 \partial_y \eta + \mu \partial_t^2 \eta = [p(x, y, 0, t)] , \quad (8)$$

iii) boundary conditions

$$\vec{v} = \begin{cases} \vec{0} & \text{on rigid wall} \\ (0, 0, \alpha \partial_t \eta) & \text{on BM} \\ (\partial_t \eta_s, 0, 0) & \text{on stapes footplate .} \end{cases} \quad \begin{matrix} (9a) \\ (9b) \\ (9c) \end{matrix}$$

The initial conditions to be used are that the motion starts rest at $t=0$. In (7a), $\nabla \xi^2 = \epsilon^2 \partial_x^2 + \partial_y^2 + \partial_z^2$. In (8), $D_2 = D_2^*/D_{2C}$ and $\mu = \mu^*/\mu_C$. Also,

$$\delta^2 = \frac{\tau t_C}{B^2}, \quad \epsilon = \frac{B}{L}, \quad \text{and } \alpha = \frac{\rho B}{\mu_C}.$$

The last parameter is simply the ratio of the mass of the fluid above the basilar membrane to the characteristic mass of the plate. As for ϵ , it is the ratio of the width to length of the BM and it is relatively small (e.g., for humans $\epsilon \sim 10^{-2}$). This is used later to derive a slender body approximation to the solution of the problem. The parameter δ is the inverse of the Reynolds number, where the latter is based on the cross-sectional width of the chamber. This too is relatively small and, accordingly, viscous boundary layer theory will be used to reduce the above problem.

The reduction of the transient problem consists of two steps. First, viscous boundary layer theory is used to reduce the fluid problem. From this, rather than solving (7), we only need to solve Laplace's equation for the pressure, where the viscosity contributes through a modified boundary condition. This reduced problem is then solved using a slender body approximation based on the fact that

$\epsilon \ll 1$.

BOUNDARY LAYER APPROXIMATION

The frequencies in the hearing range are fairly high, for example, they range from about 20 to 20,000 Hz for the human ear. This serves as the basis for the first reduction of the equations of motion and involves the application of viscous boundary layer theory. In the approximations to follow it is assumed that $\delta \ll 1$. Also, in the discussion the other parameters in the problem are assumed fixed. The analysis splits naturally into three parts, the first two involve deriving the approximations for the inviscid and boundary layer regions and the third step deals with their matching. The details are somewhat involved but they result in a considerable reduction of the fluid equations. For those who may wish to skip the derivation, the conclusions of the analysis are given in the last paragraph of this section.

i) Inviscid Region: In the inviscid core the appropriate expansions of the fluid velocity and pressure are

$$\vec{v} \sim \vec{v}_0(x, y, z, t) + \delta \vec{v}_1 + \dots , \quad (10a)$$

and

$$p \sim p_0(x, y, z, t) + \delta p_1 + \dots . \quad (10b)$$

Substituting these into (7) and equating like powers of δ leads to the following problem for the n th term in the expansion

$$O(\delta^n) \quad \nabla^2 p_n = 0$$

$$\partial_t \vec{v}_n = -\nabla p_n . \quad (11)$$

As expected it is, in general, not possible to satisfy all of the boundary conditions with this approximation (in particular, the no-slip condition in (9) can not be satisfied). This necessitates

the introduction of a boundary layer.

ii) Boundary Layer: To obtain the boundary layer approximation only the layer above the partition is considered. The analysis for the rest of the cochlear wall is similar and involves the introduction of orthogonal coordinates orientated with respect to the normal direction (Holmes and Cole, 1984). For the region above the partition the boundary layer coordinate is

$$\tilde{z} = z/\delta . \quad (12)$$

The Navier-Stokes equations (7) in this case take the form

$$[\partial_t - \partial_{\tilde{z}}^2 - \delta^2 \nabla_{x,y}^2] \vec{v} = -\left[\partial_x, \partial_y, \frac{1}{\delta} \partial_{\tilde{z}}\right] p , \quad (13a)$$

$$\partial_{\tilde{z}} v_3 + \delta (\epsilon^2 \partial_x v_1 + \partial_y v_2) = 0 \quad (13b)$$

where

$$\nabla_{x,y}^2 = \epsilon^2 \partial_x^2 + \partial_y^2 .$$

The appropriate expansions in this layer are

$$\vec{v} \sim \vec{v}_0(x, y, \tilde{z}, t) + \delta \vec{v}_1 + \dots , \quad (14a)$$

and

$$p \sim P_0(x, y, \tilde{z}, t) + \delta P_1 + \dots . \quad (14b)$$

Proceeding as before, by substituting these into (13) and equating like powers of δ the following problems are obtained:

$$O(1) \quad \partial_{\tilde{z}} P_0 = 0$$

$$\partial_{\tilde{z}} v_{30} = 0$$

$$[\partial_t - \partial_{\tilde{z}}^2] v_{50} = - \partial_s P_0 , \quad (s = x, y) .$$

Solving these equations and using boundary condition (9b) one finds that

$$P_0 = P_0(x, y, t) ,$$

$$V_{30} = \alpha \partial_t \eta_0 ,$$

and

$$V_{50} = - \int_0^t \operatorname{erf} \left[\frac{\tilde{z}}{2\sqrt{t-\tau}} \right] \partial_s P_0 d\tau , \quad (s=x, y) .$$

To obtain a uniformly valid two term approximation it is necessary to solve for at least some of the second terms in the expansion.

$$0(8) \quad \partial_z V_{31} = - \alpha \partial_t^2 \eta_0$$

$$\partial_z V_{51} = \int_0^t \operatorname{erf} \left[\frac{\tilde{z}}{2\sqrt{t-\tau}} \right] \nabla_{x,y}^2 P_0 d\tau .$$

Using the Laplace transform one finds that the solutions of the above problems are

$$P_1 = -\alpha \tilde{z} \partial_t^2 \eta_0 + b(x, y, t)$$

and

$$V_{31} = \alpha \partial_t \eta_1 + \int_0^t \left[\tilde{z} - 2\sqrt{t-\tau} \left[\frac{1}{\sqrt{\pi}} - i \operatorname{erfc} \left(\frac{\tilde{z}}{2\sqrt{t-\tau}} \right) \right] \right] \nabla_{x,y}^2 P_0 d\tau ,$$

where b is a constant of integration.

iii) Matching: It remains to match the expansions from the two regions and to do so an intermediate variable is used, which is defined as

$$\bar{z} = \frac{z}{\sqrt{\delta}} = \tilde{z} \sqrt{\delta} . \quad (15)$$

With this, using Taylor's theorem the inviscid approximation for the pressure (10b) can be written as

$$p \sim p_0 \Big|_{z=0} + \sqrt{\delta z} \partial_z p_0 \Big|_{z=0} + \delta (p_1 + \frac{1}{2} \bar{z}^2 \partial_z^2 p_0) \Big|_{z=0} + \dots , \quad (16)$$

and the boundary layer approximation (14b) is

$$p \sim p_0 - \alpha \bar{z} \sqrt{\delta} \partial_t^2 \eta_0 + \delta b + \dots . \quad (17)$$

Matching (16) and (17) as well as matching the velocities one finds

$$p_0 = p_0 \Big|_{z=0} ,$$

and

$$\partial_z p_0 \Big|_{z=0} = -\alpha \partial_t^2 \eta_0 ,$$

$$\partial_z p_1 \Big|_{z=0} = -\frac{1}{\sqrt{\pi}} \int_0^t \frac{1}{\sqrt{t-\tau}} \nabla_{x,y}^2 p_0 d\tau .$$

Combining these

$$\partial_z p_1 \Big|_{z=0} \sim -\alpha \partial_t^2 \eta_0 - \frac{\delta}{\sqrt{\pi}} \int_0^t \frac{1}{\sqrt{t-\tau}} \partial_z^2 p_0(x,y,0,t) d\tau . \quad (18)$$

Based on the above analysis, a uniformly valid two term approximation (in δ) of the fluid pressure is obtained by solving

$$\nabla_x^2 p = 0 , \quad (19)$$

where, for $0 < x < 1$,

$$\partial_n p - \frac{\delta}{\sqrt{\pi}} \int_0^t \frac{1}{\sqrt{t-\tau}} \partial_n^2 p d\tau = \begin{cases} 0 & \text{on rigid wall} \\ \alpha \partial_t^2 \eta & \text{on BM} . \end{cases} \quad (20a)$$

In (20a), n is the unit outward normal to the cochlear wall. A similar condition applies at the basal end ($x=0$) and is given as

$$\partial_x p + \frac{\epsilon \delta}{\sqrt{\pi}} \int_0^t \frac{1}{\sqrt{t-\tau}} \partial_x^2 p d\tau = - \partial_t^2 n_s . \quad (20b)$$

Therefore, the original equations for the fluid (7) along with boundary conditions (9) have been replaced with (19) and (20). In other words, it remains to only solve one equation for the fluid and the viscosity now only contributes in the boundary condition, rather than in the equation of motion. It is also of interest to note that this approximation reduces to the one derived earlier by Holmes and Cole (1984) for the longtime periodic response to a pure-tone forcing as $t \rightarrow \infty$. Moreover, it reduces to the transient low frequency approximation used in Holmes (1981, 1982) in the case of a low frequency signal.

SOLUTION OF REDUCED PROBLEM

It remains to solve the reduced fluid equations derived in the last section in conjunction with the plate equation and associated boundary conditions. There are a number of ways to do this and the one to be used here involves the Fourier transform in t . For a variable such as $\eta(x, y, t)$ its transform, which is represented with a capital $N(x, y, \omega)$ as well as by the symbol $\mathcal{F}(\eta)$, is defined as

$$N(x, y, \omega) = \frac{1}{\sqrt{2\pi}} \int_{-\infty}^{\infty} \eta(x, y, t) e^{-i\omega t} dt .$$

To be able to transform the equations of motion it is necessary to assume that the Fourier transform of the stapes displacement is well defined. With this the transformation of the problem is fairly straightforward, except perhaps for the convolution integral in boundary conditions (20). The latter can be evaluated by interchanging the orders of integration as follows

$$\begin{aligned} \mathcal{F} \left(\int_0^t \frac{1}{\sqrt{t-\tau}} \partial_n^2 p d\tau \right) &= \frac{1}{\sqrt{2\pi}} \int_0^{\infty} \int_0^t \frac{1}{\sqrt{t-\tau}} \partial_n^2 p e^{-i\omega t} d\tau dt \\ &= \frac{1}{\sqrt{2\pi}} \int_0^{\infty} \int_{\tau}^{\infty} \frac{1}{\sqrt{t-\tau}} \partial_n^2 p e^{-i\omega t} dt d\tau \\ &= \frac{1}{\sqrt{2\pi}} \int_0^{\infty} \int_0^{\infty} \frac{1}{\sqrt{r}} \partial_n^2 p e^{-i\omega(r+\tau)} dr d\tau \\ &= \sqrt{\frac{\pi}{i\omega}} \partial_n^2 P . \end{aligned}$$

With this the fluid equation (19) transforms as

$$\nabla_t^2 P = 0 , \quad (21)$$

and equation (8) for the BM is

$$(D_2 \partial_y - \omega^2 \mu) N = -2P(x, y, 0, \omega) , \quad (22)$$

where, from (20a),

$$\partial_n P - \frac{\delta}{\sqrt{i\omega}} \partial_n^2 P = \begin{cases} 0 & \text{on rigid wall} \\ -\alpha \omega^2 N & \text{on BM} \end{cases}$$

and, from (20b),

$$\partial_x P + \frac{\epsilon \delta}{\sqrt{i\omega}} \partial_x^2 P = \omega^2 N_s \quad \text{on stapes footplate} .$$

This problem is essentially the same as the one studied in Holmes and Cole (1984). Consequently, it is possible to simply write down a first term approximation of the solution. This approximation, which is based on the assumption that $\epsilon \ll 1$, is derived using a multiple scale argument. The result is that the solution for the (transformed) BM displacement has the form

$$N \sim \frac{\epsilon}{\alpha} A(x, \omega) e^{-i\theta(x, \omega)} n_0(x, y) . \quad (23)$$

The functions in this expression, such as $A(x, \omega)$, will be given later as they are not needed to complete the derivation of the solution of the problem. Inverting (23) using the convolution theorem leads to

$$n \sim \frac{1}{\sqrt{2\pi}} \int_0^\infty K_0(x, y, t-\tau) n_s(\tau) d\tau , \quad (24a)$$

where

$$K_0(x, y, t) = \mathcal{F}^{-1} \left[\frac{\epsilon}{\alpha} A(x, \omega) e^{-i\theta(x, \omega)} \right] n_0(x, y) . \quad (24b)$$

Note that it has been assumed in (24) that $n = 0$ for $t \leq 0$ and the function n_0 is independent of ω .

It remains to invert the inverse Fourier transform in (24b). However, because of the relatively complicated nature of the functions there is no apparent closed form inversion. Nevertheless, there are some simplifications that can be made. For example, since A is an odd function of ω and $\theta(x, -\omega) = -\theta(x, \omega) + \pi$ then it is only necessary to integrate over $0 < \omega < \infty$ in (24b).

SOLUTION OF TRANSIENT PROBLEM

In the last two sections the original equations of motion were reduced and a first term approximation to the transient problem was derived. The result is that the displacement of the basilar membrane is given as

$$\eta^*(x, y, t) \sim \int_0^\infty K(x, y, t-\tau) \eta_s^*(\tau) d\tau , \quad (25a)$$

where

$$K(x, y, t) = \frac{1}{\pi} \int_0^\infty A(x, \omega) \cos\{\omega t - \theta(x, \omega)\} d\omega + \eta_0(x, y). \quad (25b)$$

The amplitude $A(x, \omega)$ and the phase $\theta(x, \omega)$ are given in (A18) and (A19), respectively. The function η_0 , which is the displacement of the wave in the transverse cross-section of the BM, is given in (A9). The time history of the displacement of the BM, as given in (25), is in the form of a convolution integral. Because of the complexity of the functions in (25b) it appears to be necessary to evaluate (25) numerically. However, the kernel defined in (25b) needs to be calculated only once. To do so for a given x and ω one must find the solution of a transcendental equation (A10), called the dispersion relation, for the local inviscid wave number k_0 . Once $k_0(x, \omega)$ is known then it is a relatively simple matter to calculate A and θ from the formulas given in the Appendix.

In the calculations to follow for the human ear the kernel is evaluated at 100 equally spaced points along the x -axis, at 50 equally spaced frequencies between 0 and 500 Hz, and at 50 logarithmically spaced frequencies between 500 and 15,000 Hz. The methods used to evaluate the kernel are the same as used in Holmes and Cole (1984) and Holmes (1986). The reason the frequency

spacing is divided in this way is because of the effects of the low frequency modes (Holmes, 1985). In particular, the amplitude and phase functions are not monotonic for low frequencies so it is necessary to increase the number of points in this region so interpolated integration can be used in (25b). By doing this, it takes about 85 sec of cpu time on an IBM 3081D to calculate the amplitude and phase functions in (25b).⁺

⁺The FORTRAN programs, and documentation, used to calculate the solution of the transient problem are available upon request from the author.

APPLICATION TO THE HUMAN COCHLEA

The transient response of the basilar membrane is now illustrated by evaluating (25) for the human ear. To do so the values used for the fluid kinematic viscosity and density are $\nu=0.008 \text{ cm}^2/\text{sec}$ and $\rho=1.0 \text{ gm/cm}^3$. For the basilar membrane $L=3.5 \text{ cm}$, the transverse bending rigidity is

$$D_2^* = \frac{E_2(h^*)^3}{12(1-\sigma^2)} ,$$

the mass density is

$$\mu^* = \mu_0 \rho h^* ,$$

and the thickness is

$$h^* = h_0^*(1-h_5x) ,$$

where $E_2=10^7 \text{ dyn/cm}^2$, $h_0^*=0.74 \times 10^{-3} \text{ cm}$, $h_5=0.38$, $\sigma=1/2$, and $\mu_0=17$. The longitudinal boundaries of the BM are $y^*=\pm BG(x)$, where $B=0.05 \text{ cm}$ and

$$G(x) = \frac{1}{12} (5x + 1) , \quad \text{for } 0 < x < 1 .$$

Also, the transverse cross-section of the cochlea chamber is rectangular with a constant area of 0.01 cm^2 and the area of the stapes footplate is 0.03 cm^2 . These values are the same as used when studying the response to a pure tone (Holmes, 1986) and are representative of the measured values for the human ear.

The forcing function to be considered is a tone-pip in which the displacement of the stapes has the form

$$\eta_s^* = \eta_{s0} \eta_s(t^*), \text{ for}$$

$$\eta_s = \begin{cases} \frac{1}{2} [1 - \cos(\omega^* t^*)] & \text{if } 0 \leq t^* \leq t_0^* \\ 0 & \text{if } t_0^* \leq t^* , \end{cases} \quad (26)$$

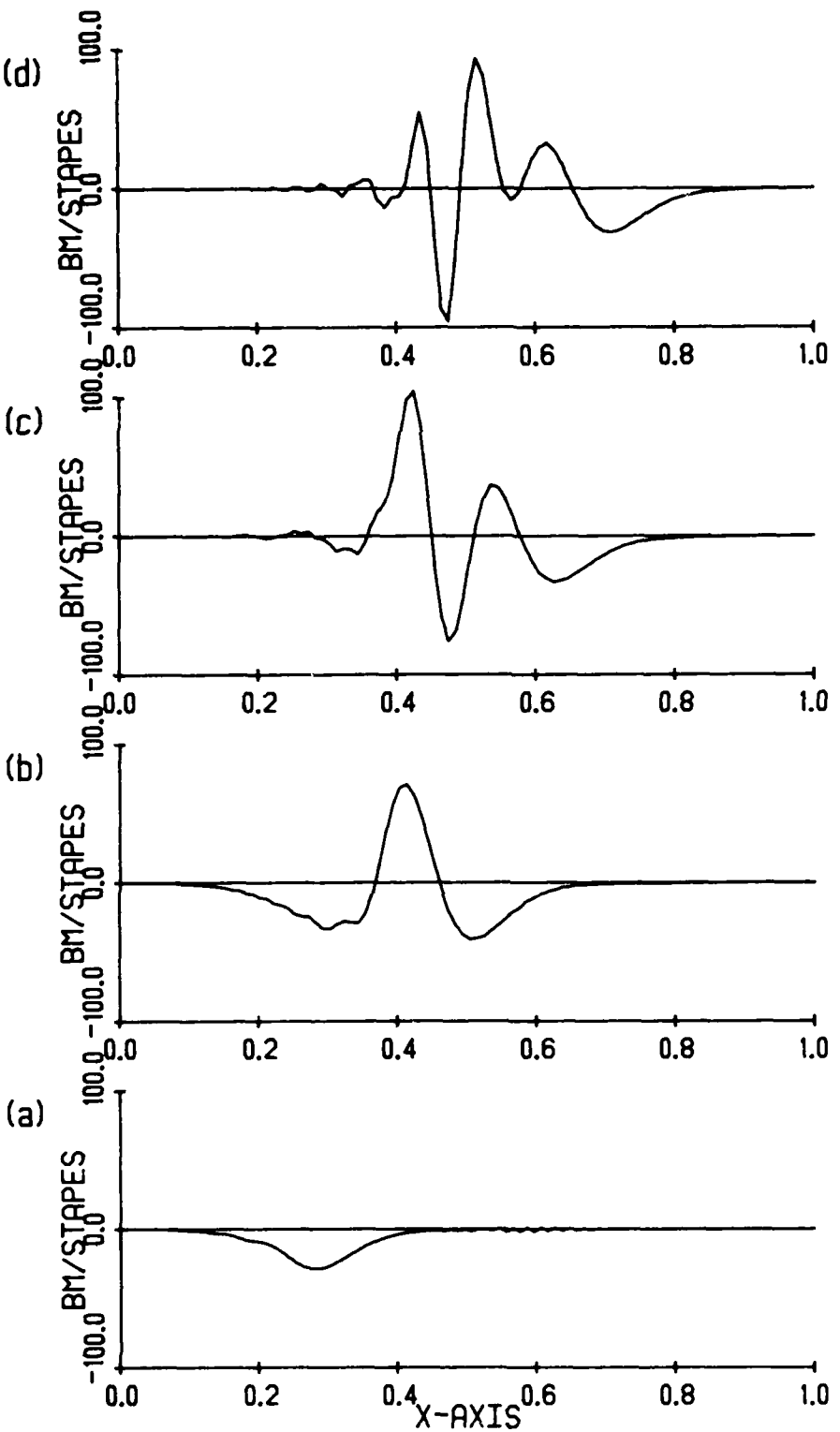


Fig. 2. The displacement of the basilar membrane in response to a tone-pip with frequency 1400 Hz at time a) 0.357, b) 1.07, c) 1.79, and d) 2.5 msec. The displacement is determined from (27) and normalized by the amplitude of the stapes.

where $t_0^* = 2n\pi/\omega^*$ and n is an integer. Inserting this into (25) and integrating one finds that

$$\eta^*(x, 0, t) \sim \frac{\eta_{50}}{\pi} \int_0^\infty \frac{\omega_0^2}{\omega(\omega_0^2 - \omega^2)} A(x, \omega) \cos[\omega t - \theta(x, \omega) - \frac{1}{2}\omega t_0] \sin\left(\frac{1}{2}\omega t_0\right) d\omega \quad (27)$$

where $t_0 = t_0^*/t_C$ and $\omega_0 = t_C\omega^*$. The numerical evaluation of this integral in the case of when $f=1400$ Hz and $n=2$ is shown in Fig. 2 at four successive times. It is seen in this figure that the initial response of the BM is in the form of a traveling wave that propagates towards the apical end. The wave takes approximately 9 msec to transverse the BM. Also note that it is the low frequency components of the disturbance that reach the apical end and they travel faster, and farther, than the higher frequency waves. This is not unexpected given the dependence of the phase velocity on frequency (Holmes, 1986).

The time histories of the displacement of the BM at three spatial locations are shown in Fig. 3 using the same signal as in Fig. 2. In each case there is a time delay before the BM begins to move. To measure this, the latency is defined as the time until the displacement reaches its first significant positive peak. This choice is made because it approximates the value measured neurally, although the latter also includes other sources of delay. In any case, as seen in Fig. 3 the time it takes the wave to reach $x=0.25$ (approximately 0.85 msec) is less than it takes it to propagate from $x=0.5$ to $x=0.75$ (which takes about 2.9 msec). This is due to the monotonic decrease of the phase velocity

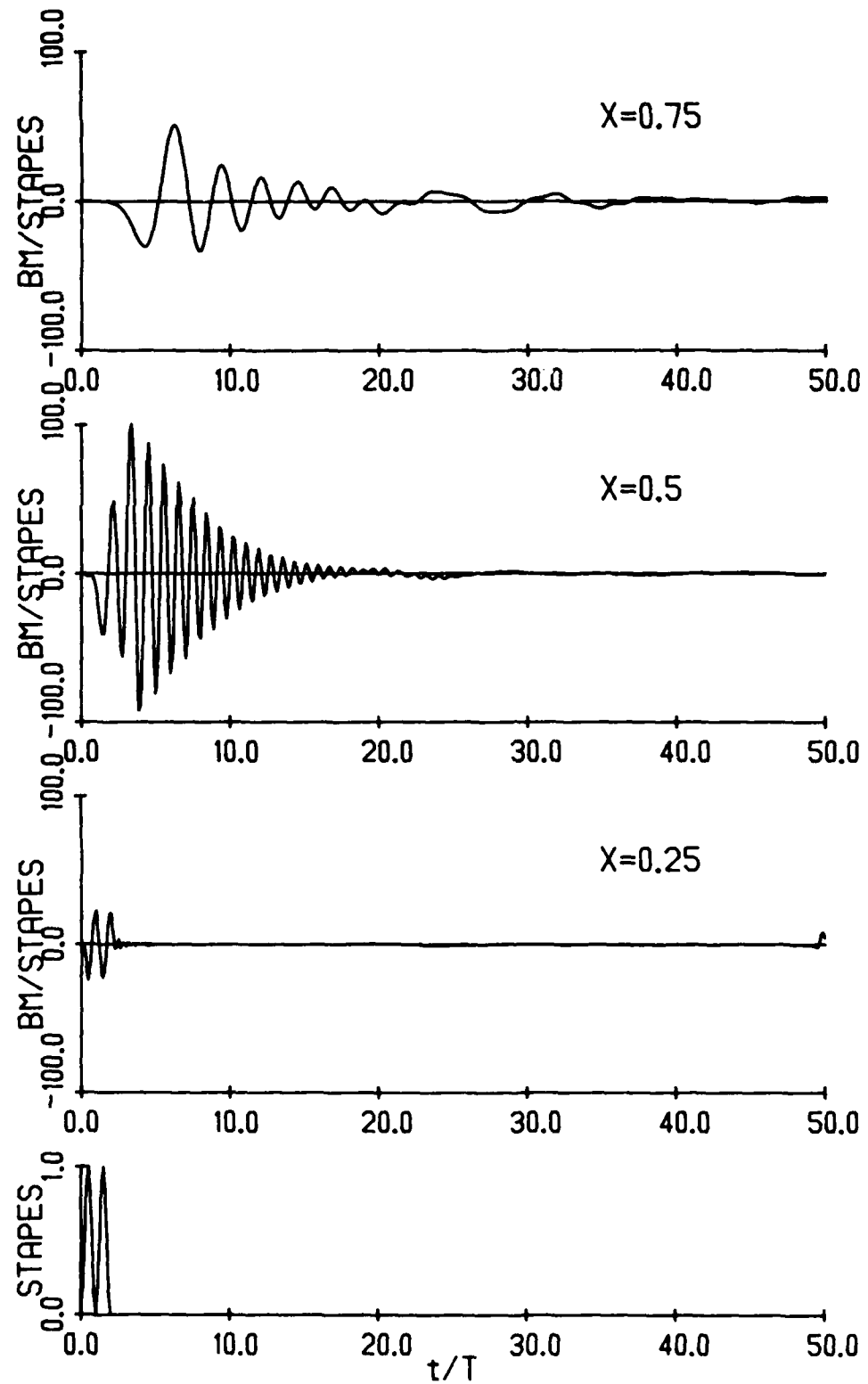


Fig. 3. Transient response of the basilar membrane at three spatial locations for a tone-pip with frequency 1400 Hz. The time axis is normalized by the period T of the forcing function.

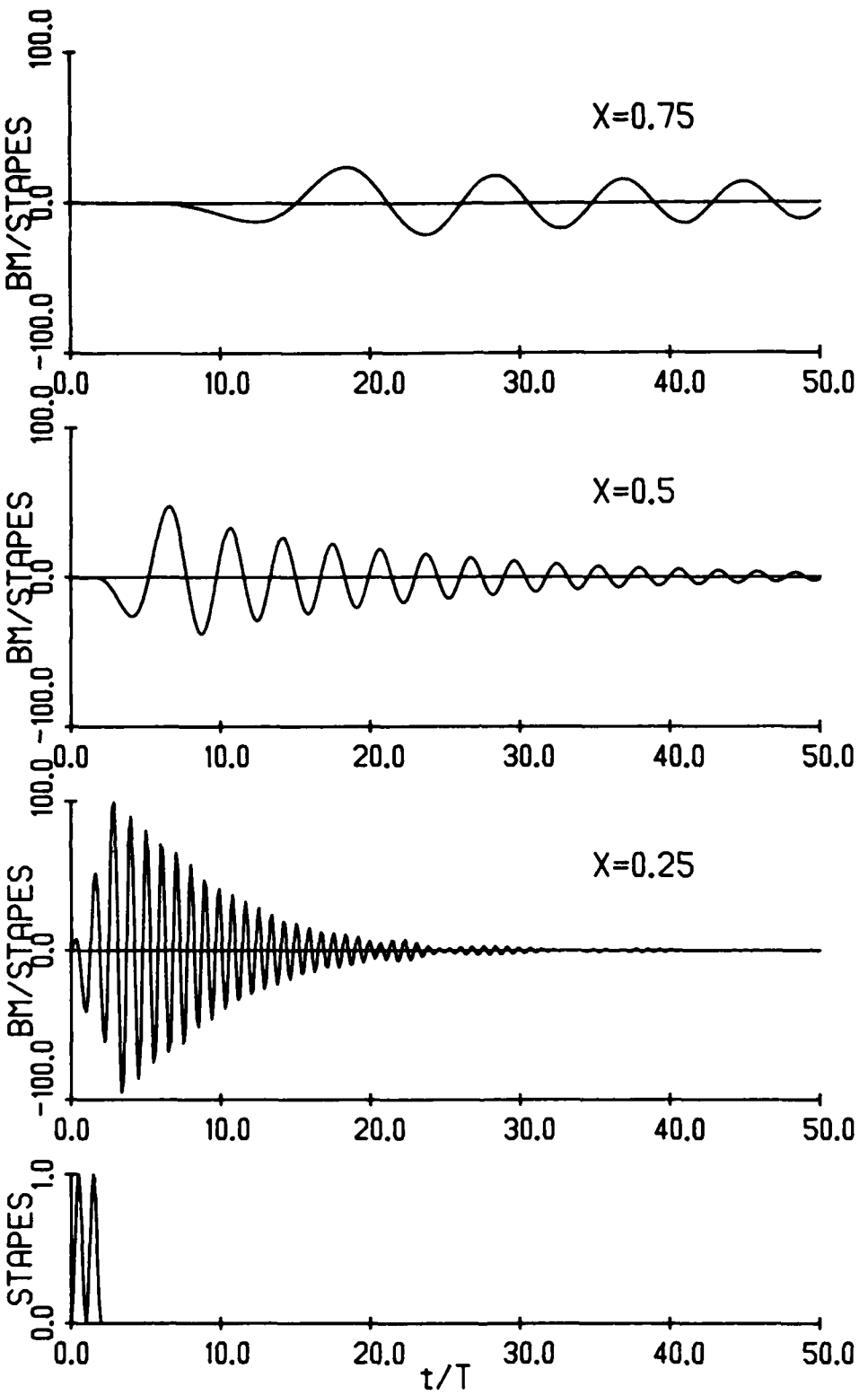


Fig. 4. Transient response of the basilar membrane at three spatial locations for a tone-pip with frequency 4570 Hz. The time axis is normalized by the period T of the forcing function.

with longitudinal position (Holmes, 1986). Something else that is seen in this figure is that the BM oscillates much more at the point $x=0.5$ than at the other two locations. The reason for this is because the characteristic frequency for $x=0.5$ is 1400 Hz. If the driving frequency is 4570 Hz, which is the characteristic frequency for $x=0.25$ then, as seen in Fig. 4, the oscillations occur at $x=0.25$ rather than at $x=0.5$.

A contour plot for the displacement of the basilar membrane is shown in Fig. 5 for the same signal that was used for Figs. 2 and 3. Only positive displacements are shown in this figure because of their importance in the depolarization of the hair cell (Bell and Holmes, 1986). In any case, the wave-like nature of the response is clearly seen along with the ringing that occurs due to the effects of the characteristic frequency. The "chain of islands," which run from the lower left to upper right, correspond to individual wave packets propagating down the basilar membrane. Except for the lower two, these chains are parallel. Also, each succeeding chain is smaller than the previous one but $x=0.5$ remains at, or near, the center of each. The contributions of the low frequencies appear primarily in the two lower packets and even then they are confined principally to the first. This is due to the start up of the signal which contains frequencies throughout the spectrum.

In the case of a pure tone signal it is possible to determine the length of time it takes for the longtime periodic solution to appear. With a forcing such as given in

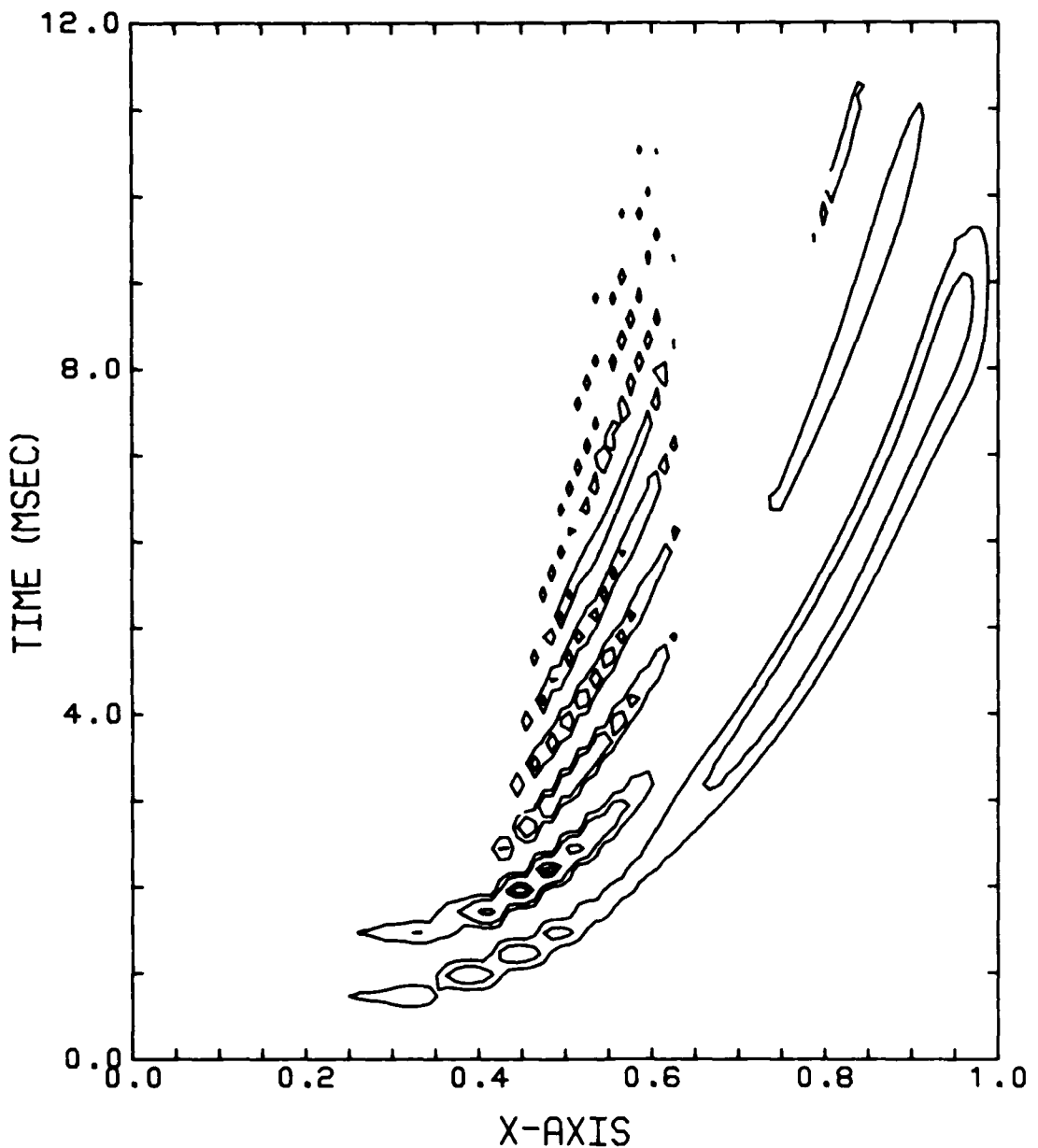


Fig. 5. The level contours for the positive displacement of the basilar membrane, normalized by the amplitude of the stapes, in response to a tone-pip with frequency 1400 Hz. The curves represent constant normalized displacements of 10, 20, 40, and 80.

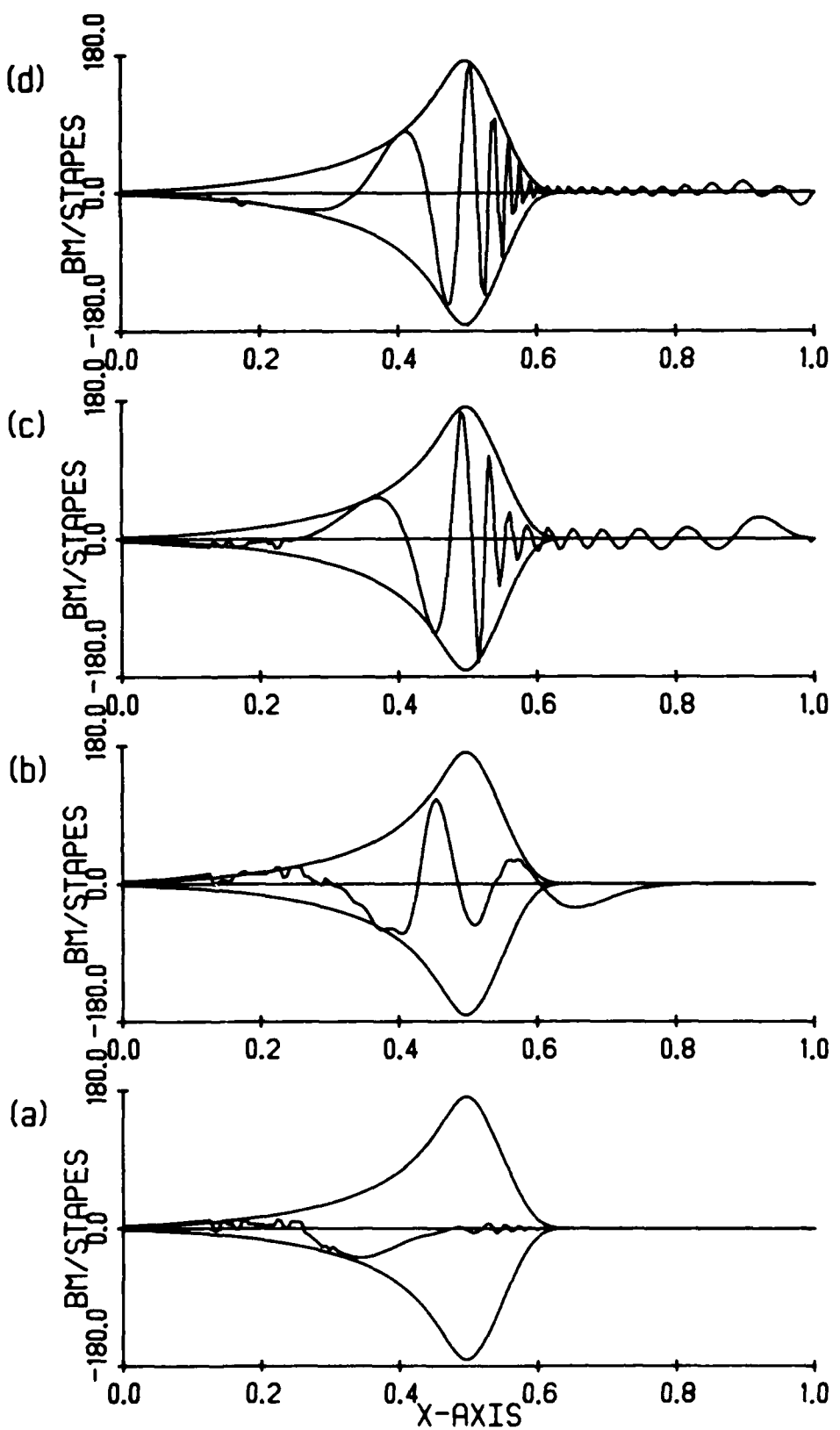


Fig. 6. Transient response of the basilar membrane for a pure-tone signal with frequency 1400 Hz, at time a) 0.5, b) 2.0, c) 8.0, and d) 16 msec. Also shown is the envelope of the corresponding longtime solution.

(26) this is the time it takes the transients associated with the start-up of the signal to propagate down the basilar membrane and decay. Based on the discussion in the earlier paragraphs this is approximately 5 msec for the higher frequency components and about 10 msec for the lower frequencies. The solution as calculated from (27) and the envelope of the longtime solution are shown in Fig. 6 at four successive times in the case of when $f=1400$ Hz and $n=50$. As expected, at the earliest time there are still appreciable transient effects, the higher frequency transients have disappeared at the three later times and the lower frequencies have effectively decayed at the last two.

Before leaving this example the method used to calculate the solution should be explained. With the earlier evaluation of the amplitude and phase functions in (25b) the integral in (25a) is evaluated using Simpson's rule with 400 equally spaced points between 0 and 15,000 Hz. This is done using the values for the amplitude and phase functions calculated earlier, which were evaluated at a smaller number of frequency points, by using linear interpolation. In doing this it takes approximately 10 sec of cpu time to calculate all of the curves shown in Fig. 3.

DISCUSSION

The method that has been used here to solve the transient problem is based on the spectral decomposition of the sound signal using the Fourier transform. By doing this the transformed problem is essentially the same as the one for the longtime response to a pure-tone, so, the solution is relatively easy to obtain. The factor that complicated the analysis was the viscous boundary layer as it was necessary to derive an approximation that described the development of the layer in time. Once this has been done the solution to the transient problem is in the form of a convolution integral in which the kernel is determined completely from the response for a pure-tone.

Although the analysis used to obtain the solution is straightforward it is necessary to evaluate the integral numerically. By comparison, for the low frequency theory the solution is simple enough that it is relatively easy to derive the characteristics of the response of the basilar membrane (Holmes, 1981). Nevertheless, the calculations used to evaluate (25) are not particularly difficult and lead to some interesting conclusions. For example, for the human cochlea the time scale associated with the development of a pure tone is about 10 msec. The decay of the displacement of the basilar membrane is also strongly dependent on the spectrum of the signal. Even in the case of a pure tone-pip lasting two cycles the basilar membrane at the characteristic place vibrates through 10 or 15 cycles. Although there are no direct experimental measurements to compare with,

responses similar to the ringing seen in the model have been observed both in the displacement of the BM as well as in the neural response (Robles, et al, 1976; Pfeiffer and Kim, 1972). Robles, et al also observed that the latency, or time delay, of the response to reach $x=0.1$ in the squirrel monkey is about 0.35 msec. The model predicts that at the same point for the human the delay is only about 0.06 msec. It is not clear why there is so much difference between the two. The theory also predicts that the total time it takes the response to reach the apical end is about 7.75 msec. From neural measurements the travel time appears to be between 7 and 8 msec for the squirrel monkey (Anderson, et al, 1971), for the chinchilla (Siegel, et al, 1982), and for the cat (Kim and Molnar, 1979). So, for this the model is in reasonable agreement with experiment. It remains though to either extend the model to account for the hair-cell system, or for direct experimental observations of the transient motion of the BM, before a more complete comparison between theory and experiment can be made.

REFERENCES

Allen, J.B. (1977), "Two-dimensional cochlear fluid model: new results," *J. Acoust. Soc. Am.* 61, 110-119.

Anderson, D.J., Rose, J.E., Hind, J.E. and Brugge, J.F. (1971). "Temporal position of discharges in single auditory nerve fibers within the cycle of a sine-wave stimulus: frequency and intensity effects," *J. Acoust. Soc. Am.* 49, 1131-1139.

Bell, J. and Holmes, M.H. (1986). "A nonlinear model for transduction in hair cells," accepted for publication in *Hearing Res.*

Holmes, M. H. (1981), "A hydroelastic model of the cochlea: an analysis for low frequencies," in Mathematical Modeling of the Hearing Process (M. H. Holmes and L. A. Rubenfeld, eds), Springer-Verlag Lecture Notes in Biomathematics, Springer-Verlag, New York, 55-69.

Holmes, M. H. (1982), "Study of the transient motion in the cochlea," *J. Acoust. Soc. Am.* 69, 751-759.

Holmes, M. H. (1985), "Frequency Discrimination in the Mammalian Cochlea," RPI Math Report 150, Rensselaer Polytechnic Institute, Troy, NY.

Holmes, M. H. (1986), "Frequency discrimination in the mammalian cochlea: theory vs experiment," submitted for publication.

Holmes, M. H. and Cole, J. D. (1983), "Cochlear Mechanics: Analysis for a Pure Tone," RPI Math Report 139, Rensselaer Polytechnic Institute, Troy, NY.

Holmes, M. H. and Cole, J. D. (1984), "Cochlear mechanics: analysis for a pure tone," *J. Acoust. Soc. Am.* 76, 767-778.

Kim, D.O. and Molnar, C.E. (1979). "A population study of cochlear fibers: comparison of spatial distributions of average-rate and phase-locking measures of responses to single tones," *J. Acoust. Soc. Am.* 42, 16-30.

Lekhnitskii, S. G. (1968), Anisotropic Plates, Gordon and Beach, New York.

Pfeiffer, R. and Kim, D. O. (1972), "Response patterns of single cochlear nerve fibers to click stimuli: description for cat," *J. Acoust. Soc. Am.* 52, 1669-1677.

Rabbitt, R. and Holmes, M. H. (1985), "Formulation and analysis of a dynamic fiber composite continuum model of the tympanic membrane," Peripheral Auditory Mechanisms (J.B. Allen, J.L. Hall, S.T. Neely, and A. Tubis, eds), Springer-Verlag, New York, 28-35.

Robles, L., Rhode, W. S. and Geisler, C. D. (1976), "Transient response of the basilar membrane measured in squirrel monkeys using the Mossbauer effect," *J. Acoust. Soc. Am.* 59, 926-939.

Siegel, J.H., Kim. D.O. and Molnar, C.E. (1982). "Effects of altering organ of Corti on cochlear distortion products f_2-f_1 and $2f_1-f_2$," *J. Neurophys.* 47, 303-328.

Stapells, D. R., Picton, T. W. and Smith, A. D. (1982), "Normal hearing thresholds for clicks," *J. Acoust. Soc. Am.* 72, 74-79.

APPENDIX. EVALUATION OF THE KERNEL FUNCTION

Once the transient problem is reduced using viscous boundary layer theory, and then Fourier transformed, it is essentially the same one found for the pure-tone response. For the latter, to obtain the displacement of the basilar membrane it is necessary to solve a nonlinear eigenvalue problem for the local inviscid wavenumber k_0 (Holmes and Cole, 1984; Holmes, 1986). This problem is given by the following partial differential equation for the (nondimensionalized) displacement of the basilar membrane in the transverse cross-section

$$(D_2 \partial_y^4 - \omega^2 \mu) \eta_0 = -2\omega^2 p_0(x, y, 0), \quad (A1)$$

where $D_2 = h^3(x)$ and $\mu = h(x)$. The function $p_0(x, y, z)$ comes from the fluid pressure and is given as

$$p_0(x, y, z) = \sum_{m=0}^{\infty} \bar{p}_m \cosh \lambda_m (H-z) \cos \gamma_m y, \quad (A2)$$

where

$$\bar{p}_m = \frac{-\alpha c_m}{\lambda_m \sinh \lambda_m H} \int_{-G}^G \eta_0(x, s) \cos \gamma_m s ds, \quad (A3)$$

$$\lambda_m^2 = \gamma_m^2 + k_0^2, \quad \gamma_m = \frac{m\pi}{H},$$

and

$$c_m = \begin{cases} \frac{1}{2H} & \text{if } m = 0 \\ \frac{1}{H} & \text{if } m \neq 0 \end{cases}.$$

Inserting (A2) into (A1) the problem that remains to be solved is

$$(D_2 \partial_y^4 - \omega^2 \mu) \eta_0 = \sum_{m=0}^{\infty} a_m \cos \gamma_m y \int_{-G}^G \eta_0(x, s) \cos \gamma_m s ds, \quad (A4)$$

where

$$a_m = \frac{2\omega^2 c_m}{\lambda_m \tanh \lambda_m H} .$$

To solve (A4) we expand η_0 in beam modes as follows

$$\eta_0(x, y) = \sum_{n=1}^{\infty} b_n(x) u_n(x, y) . \quad (A5)$$

The functions $u_n(x)$ are the natural modes of the simply supported elastic beam in the transverse cross-section and are given as

$$u_n(x, y) = \frac{\cos(r_n y)}{\sqrt{G(x)}} , \quad (A6a)$$

where

$$r_n = \frac{(2n-1)\pi}{2G(x)} . \quad (A6b)$$

Substituting (A5) into (A4), and using the orthogonality of the modes, the following system of equations is obtained

$$(D_2 r_k^4 - \omega^2 \mu) b_k = \sum_n \sum_m a_m b_n K_{mn} K_{mk}, \quad k = 1, 2, \dots , \quad (A7)$$

where

$$K_{mn}(x) = \int_{-G}^G u_n(x, y) \cos(\gamma_m y) dy \quad (A8)$$

$$= \begin{cases} \frac{2(-1)^{n+1} r_n \cos \gamma_m G}{\sqrt{G} (r_n^2 - \gamma_m^2)} & \text{if } r_n \neq \gamma_m \\ \sqrt{G} & \text{if } r_n = \gamma_m \end{cases}$$

In addition to the b_k 's the above system of equations also determines the local inviscid wavenumber. In fact, the dispersion relation is the characteristic polynomial for (A7).

Up to this point all of the beam modes have been included in the representation of the solution. However, because of the

symmetry of the problem (in y) the first beam mode is all that is necessary to obtain an accurate approximation to the solution. In this case, we have from (A5) that

$$\eta_0(x, y) = \frac{\cos\left[\frac{\pi y}{2G(x)}\right]}{\sqrt{G(x)}} . \quad (A9)$$

Also, the system of equations (A7) reduces to finding the solution to the following dispersion relation for the local inviscid wavenumber k_0

$$D_2 \omega_r^2 - \omega^2 u = \sum_{m=0}^{\infty} a_m k_m^2 , \quad (A10)$$

where

$$\omega_r = \left(\frac{\pi}{2G}\right)^2 .$$

Once k_0 is determined from (A10) the amplitude $A_r(x, \omega)$ and the phase $\theta_r(x, \omega)$ of the right-traveling wave are given by

$$A_r = \frac{A_0}{\sqrt{k_0 \int \int p_0^2 dy dz}} \cdot e^{-\frac{B_0}{\epsilon} \int_0^x k_1 ds} , \quad (A11)$$

and

$$\theta_r = \frac{\pi}{2} + \frac{1}{\epsilon} \int_0^x (k_0 + B_0 k_1) ds , \quad (A12)$$

where

$$\int \int p_0^2(x, y, z) dy dz = \frac{1}{2} H \sum_{m=0}^{\infty} \bar{P}_m^2 L_{mm} , \quad (A13)$$

and

$$A_0 = \frac{\pi k_0(0) A_w}{4G(0)} \sqrt{k_0(0) \int \int p_0^2(0, y, z) dy dz} . \quad (A14)$$

The function $k_1(x)$ in (A11), (A12) represents the viscous contribution to the wave number and is given as

$$k_1(x) = \frac{1}{k_0(x)} \left[\frac{H \sum_{m=0}^{\infty} \lambda_m^2 \bar{P}_m^2 (1 + \cosh^2 \lambda_m H) - \sum_{m=0}^{\infty} \sum_{n=0}^{\infty} (-1)^{m+n} \bar{P}_m \bar{P}_n \gamma_m^2 L_{mn}}{H \sum_{m=0}^{\infty} \bar{P}_m^2 L_{mm}} \right]$$

where

$$L_{mn} = \begin{cases} \frac{\sinh(\lambda_n + \lambda_m)H}{\lambda_n + \lambda_m} + \frac{\sinh(\lambda_n - \lambda_m)H}{\lambda_n - \lambda_m} & \text{if } m \neq n \\ H + \frac{\sinh 2\lambda_n H}{2\lambda_n} & \text{if } m = n \end{cases}$$
(A16)

The parameters are

$$\epsilon = \frac{B}{L}, \quad \beta_0 = \frac{\delta}{\sqrt{2i\omega t}}, \quad \alpha = \frac{\rho B}{u_c}, \quad (A17)$$

and $H(x) = H^*/B$ is the nondimensional "radius" of the cochlear fluid chamber (see Fig. 1). The constant A_w in (A14) is the nondimensional area of the stapes footplate and it is related to the actual area A_w^* as follows

$$A_w^* = B^2 A_w.$$

Finally, in (A13) the function P_m , which is defined in (A3), is

$$\bar{P}_m = \frac{-\alpha c_m K_{m1}}{\lambda_m \sinh \lambda_m H}.$$

The amplitude $A(x, \omega)$ in (25) includes A_r as well as the contributions of the waves reflected at $x=1$. To account for these let $A_g(x, \omega)$ and $\theta_g(x, \omega)$ be such that

$$A_L e^{i\theta_L} = \frac{1 - e^{2i(k - \bar{k}_1)}}{1 + e^{-2ik_1}},$$

where

$$k = \frac{1}{\epsilon} \int_0^x [k_0 + \beta_0(1-i)k_1] ds,$$

and

$$\bar{k}_1 = k \Big|_{x=1}.$$

With this

$$A(x, \omega) = A_r(x, \omega) A_L(x, \omega), \quad (A18)$$

and

$$\theta(x, \omega) = \theta_r(x, \omega) - \theta_L(x, \omega). \quad (A19)$$



A hand-drawn diagram consisting of two large circles, one on the left and one on the right. A horizontal line connects the two circles. From the center of this connecting line, a vertical line segment extends upwards to the top of the right-hand circle.

7 - 86